



## Interplay between I308 and Y310 residues in the third repeat of microtubule-binding domain is essential for tau filament formation

Keiko Naruto<sup>a</sup>, Katsuhiko Minoura<sup>a,\*</sup>, Ryouhei Okuda<sup>a</sup>, Taizo Taniguchi<sup>b</sup>, Yasuko In<sup>a</sup>, Toshimasa Ishida<sup>a</sup>, Koji Tomoo<sup>a,\*\*</sup>

<sup>a</sup> Department of Physical Chemistry, Osaka University of Pharmaceutical Sciences, 4-20-1 Nasahara, Takatsuki, Osaka 569-11, Japan

<sup>b</sup> Behavioral and Medical Sciences Research Consortium, 2-5-7 Tamachi, Akashi, Hyogo 673-0025, Japan

### ARTICLE INFO

#### Article history:

Received 30 June 2010

Revised 23 August 2010

Accepted 6 September 2010

Available online 17 September 2010

Edited by Jesus Avila

#### Keywords:

Tau

Microtubule-binding domain

Tyrosine residue

Isoleucine residue

Filament formation

C–H···π interaction

### ABSTRACT

**Investigation of the mechanism of tau polymerization is indispensable for finding inhibitory conditions or identifying compounds preventing the formation of paired helical filament or oligomers. Tau contains a microtubule-binding domain consisting of three or four repeats in its C-terminal half. It has been considered that the key event in tau polymerization is the formation of a β-sheet structure arising from a short hexapeptide <sup>306</sup>VQIVYK<sup>311</sup> in the third repeat of tau. In this paper, we report for the first time that the C–H···π interaction between Ile308 and Tyr310 is the elemental structural scaffold essential for forming a dry “steric zipper” structure in tau amyloid fibrils.**

© 2010 Federation of European Biochemical Societies. Published by Elsevier B.V. All rights reserved.

### 1. Introduction

Tau is normally found in axonal microtubules (MTs) and plays a role in the regulation of MT formation and stabilization [1]. This MT-associated tau is a highly soluble protein and shows hardly any tendency to assemble under physiological conditions. In the brains of Alzheimer's disease (AD) patients, however, tau dissociates from axonal MTs through an extensive phosphorylation and aggregates intracellularly to form an insoluble paired helical filament (PHF) called the neurofibrillary tangle [2]. Investigation of the mechanism of tau polymerization is hence indispensable for finding inhibitory conditions or identifying compounds preventing the formation of PHFs or oligomers, which may slow down or even reverse neuronal disease in AD. Tau contains a microtubule-binding domain (MBD) consisting of three or four repeats in the C-terminal half (Fig. 1), and it has been considered that the key event in

tau polymerization is the formation of a β-sheet structure arising from the short hexapeptide <sup>306</sup>VQIVYK<sup>311</sup> in the third repeat of tau [3,4]. X-ray crystal analysis [5] showed that this sequence adopts a β-strand conformation and forms parallel β-sheets with other VQIVYK sequences that combine in a face-to-face interdigitating dry “steric zipper” structure and form amyloid-like fibrils with the same cross β-structure found in full tau amyloid fibrils. To investigate the function of the Tyr310 residue in MBD filament formation, we have, recently, investigated the aggregation behavior of a series of Tyr-substituted, deleted or inserted MBD mutants and clarified the importance of Tyr located specifically at position 310 [6]. In this communication, we report for the first time that the filament formation of MBD is accomplished by the interplay between Ile308 and Tyr310, not by Tyr310 alone. This new result indicates the initial structural scaffold essential for forming a dry “steric zipper” structure in tau amyloid fibrils.

### 2. Materials and methods

#### 2.1. Chemicals

Heparin (average molecular weight = 6000) and thioflavin S (ThS) were purchased from Sigma Co. The other commercially available materials used were of reagent grade or higher.

*Abbreviations:* 3RMBD, three-repeated MBD; 4RMBD, four-repeated MBD; AD, Alzheimer's disease; CD, circular dichroism; His, histidine; EM, electron microscopy; MBD, microtubule-binding domain; MT, microtubule; PCR, polymerase chain reaction; PHF, paired helical filament; SDS–PAGE, sodium dodecyl sulfate polyacrylamide gel electrophoresis; TA, thymine adenine; ThS, thioflavin S

\* Corresponding author. Fax: +81 72 690 1068.

\*\* Corresponding author. Fax: +81 72 690 1068.

E-mail addresses: [minoura@gly.oups.ac.jp](mailto:minoura@gly.oups.ac.jp) (K. Minoura), [tomoo@gly.oups.ac.jp](mailto:tomoo@gly.oups.ac.jp) (K. Tomoo).

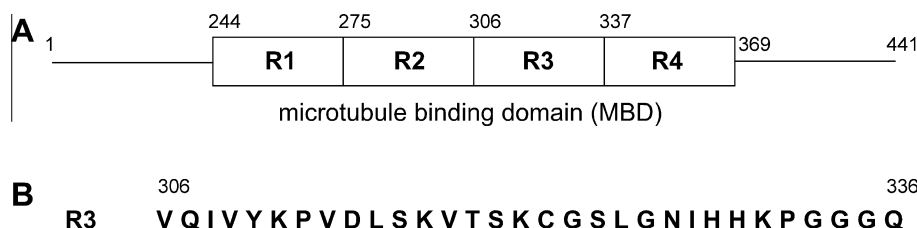


**Fig. 1.** Schematic of entire four-repeat human tau (A) and amino acid sequences of the third repeat peptide of MBD (B). The number of tau amino acid residues refers to the longest isoform of human tau (441 residues).

## 2.2. Preparation of recombinant wild 4RMBD and its Tyr or Ala-substituted mutants

The gene expression and purification of histidine (His)-tagged three-repeated MBD (3RMBD) and 4RMBD of human brain tau were performed using methods described in a previous paper [6], and the purities of these domains were confirmed by sodium dodecyl sulfate polyacrylamide gel electrophoresis (SDS–PAGE).

The Tyr or Ala-substituted genes of 4RMBD were constructed from human 2N4R by the thymine adenine cloning. After amplification by the polymerase chain reaction using a primer designed for producing each intended gene and rTaq polymerase, each gene was verified by forward and reverse dideoxy sequencings and inserted into the pET-23 vector treated with *NdeI*–*Sall* restriction enzymes and transformed into the BL21(DE3) strain. The purification of His-tagged MBD mutant was performed using a combination of cation exchange chromatography (HiPrep™ 16/10 SP–FF) [gradient method of sample solution (50 mM Tris–HCl buffer, pH 7.6) by 0–1 M NaCl] and Ni-chelating affinity chromatography (Chelating Sepharose™ Fast Flow) [binding: 50 mM Tris–HCl buffer (pH 7.6) + 0.5 M NaCl + 10 mM imidazole; elution: 50 mM Tris–HCl buffer (pH 7.6) + 0.5 M NaCl + 100 mM imidazole]. The purity of each peptide was confirmed by SDS–PAGE. The concentration of each sample was determined by measuring UV absorption at 280 nm ( $\epsilon = 1280 \text{ mol}^{-1} \text{ L cm}^{-1}$  for Tyr residue) and Bradford protein assay.

## 2.3. ThS fluorescence measurement

The 25  $\mu\text{M}$  solution of each sample was prepared using 50 mM Tris–HCl buffer (pH 7.6), and 10  $\mu\text{M}$  ThS was added to each solution. Fluorescence intensity was measured using a JASCO FP-6500 instrument with a 2 mm quartz cell maintained at 25 °C using a circulating water bath. After adding 6.25  $\mu\text{M}$  heparin (optimal concentration for aggregation) to each sample solution, the aggregation profile of each sample was monitored by plotting the time course of fluorescence intensity with excitation at 440 nm and emission at 500 nm. The background fluorescence of each sample solution was subtracted when necessary. The same measurement was repeated at least three times using newly prepared samples to confirm the reproducibility, and the averaged values were used for the data presentation.

## 2.4. Circular dichroism (CD) measurement

The 25  $\mu\text{M}$  solution of each sample was prepared using 20 mM phosphate buffer (pH 7.6). After adding 6.25  $\mu\text{M}$  heparin to each sample solution, the CD spectral change was monitored as a function of the time course of the reaction. All measurements were taken at 25 °C with a JASCO J-820 spectrometer in a cuvette with a 0.5 mm path length. For each experiment under N<sub>2</sub> gas flow, the measurement from 190 to 250 nm was repeated eight times and the results were summed. The same measurement was repeated

at least three times using newly prepared samples to confirm the reproducibility of the results. Data are expressed in terms of mean residual ellipticity  $[\theta]$  in  $\text{deg cm}^2 \text{ dmol}^{-1}$ .

## 2.5. Electron microscopy (EM) measurement

The 25  $\mu\text{M}$  solution of each sample was mixed with 6.25  $\mu\text{M}$  heparin in 50 mM Tris–HCl buffer (pH 7.6) and then incubated at 37 °C for 48 h. Copper grids (600 mesh) were used for negative-staining EM. One drop of each protein solution and one drop of 2% uranyl acetate were placed on the grid. After 1 min, excess fluid was removed from the grids. Negative-staining EM was performed using an electron microscope (Hitachi Co.) operated at 75 kV.

## 3. Results and discussion

### 3.1. Aggregation behavior of four-repeated MBD (4RMBD) mutant

The aggregation behavior of a series of 4RMBD mutants, in which each residue in the <sup>306</sup>VQIVYK<sup>311</sup> sequence was substituted with Ala or Tyr, was investigated by ThS fluorescence measurement, CD spectroscopy, and EM. The results are summarized in Table 1 and representative results are shown in Fig. 2. A considerable aggregation ability of 4RMBD was lost with Y310A mutation despite the substitution of Tyr for other residues in the <sup>306</sup>VQIVYK<sup>311</sup> sequence, except for Q307Y/ Y310A. Among them, the complete loss was observed for the I308Y/Y310A mutant. Note that the loss

**Table 1**

Changes in ThS fluorescence, CD and EM morphology of 4RMBD mutants and wild-type 4RMDA@or tau (25 mM) at 25 h after starting aggrega.

Mutant	Relative fluorescence intensity (%)	Relative change (%) of molar ellipticity at 200 nm	EM picture
Wild 4RMBD	100	100	Filament
V306Y/Y310A	0	10	Granule (+1)
Q307Y/Y310A	100	90	Filament
I308Y/Y310A	0	0	No granule and no filament
V309Y/Y310A	20	10	Granule (+2)
Y310A/K311Y	5	5	Granule (+1)
V306A/Y310	80	80	Filament
Q307A/Y310	50	30	Short filament
I308A/Y310	0	0	No granule and no filament
V309A/Y310	50	30	Short filament
K311A/Y310	90	100	Filament
Q307Y/V309A/Y310A	0	0	No granule and no filament
Wild-type tau	100	100	Filament
Y310A	0	0	No granule and no filament
I308A/Y310	0	0	No granule and no filament

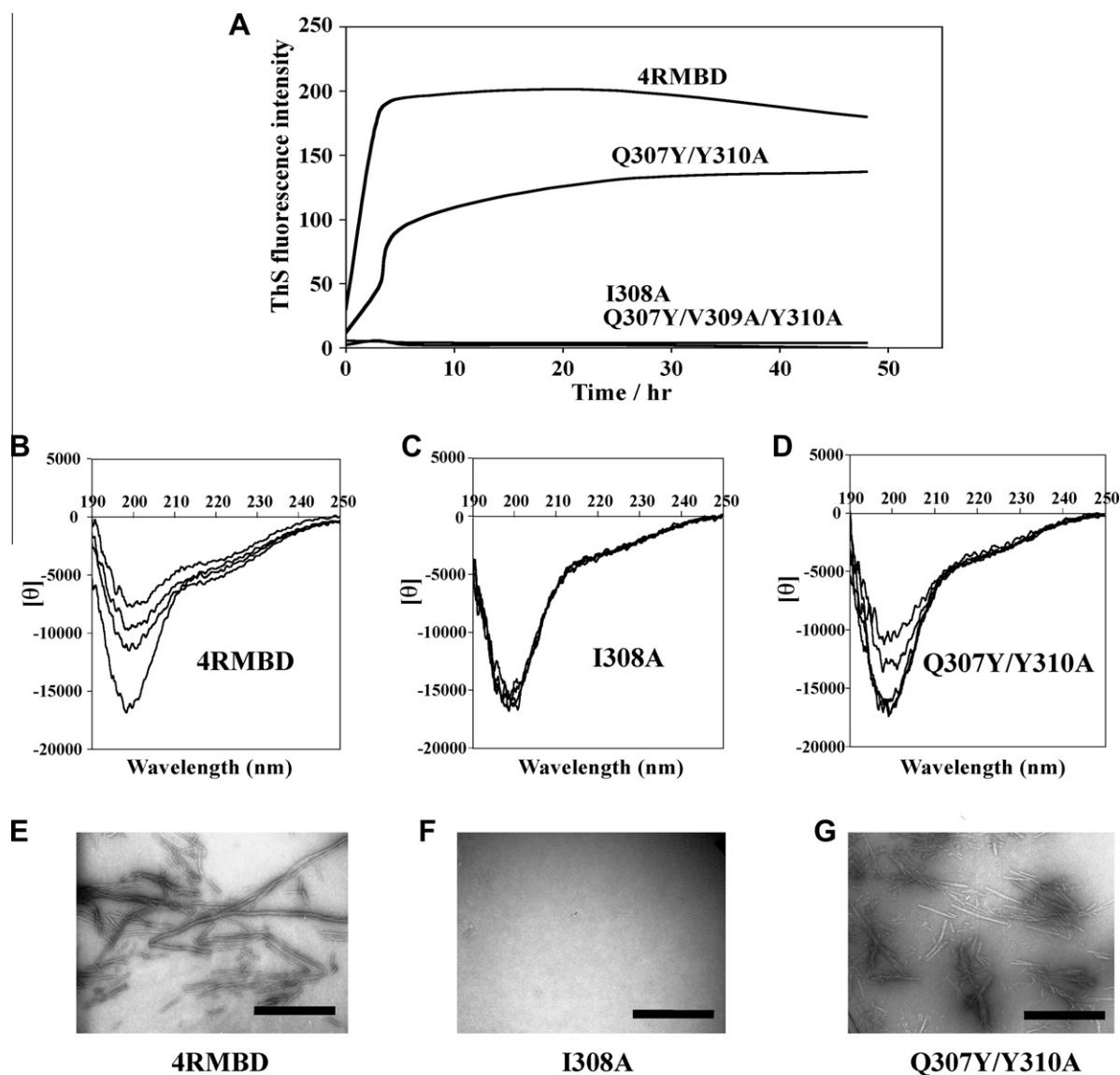


**Fig. 2.** Time-dependent ThS fluorescence intensity profiles (A), time-dependent CD spectra (B–D), and negative-staining EM images of wild 4RMBD and its I308A and Q307Y/Y310A mutants (E–G). The Q307Y/V309A/Y310A mutant shows essentially the same figures as I308A. The respective CD spectra correspond to 0 min, 3, 6, and 24 h after adding heparin to the solution (horizontal axis from bottom to top at 200 nm). The length of the bar in (E–G) corresponds to 500 nm.

of aggregation ability with Y310A mutation was also observed for 3RMBD and full-length tau, indicating that the Tyr310 in the third repeat of MBD is essential for the filament formation of tau, as reported in related studies [6–8].

In contrast, it is remarkable that the Q307Y/Y310A mutant still shows a similar aggregation profile and filament morphology to wild-type 4RMBD. This first-time observation indicates that the aggregation pathway of the Q307Y/Y310A mutant is the same as that of wild-type 4RMBD. To determine why the Q307Y/Y310A mutant exhibits such potent aggregation, the aggregation behavior of the Y310-fixed and Ala-scanned mutants for each residue in the <sup>306</sup>VQIVYK<sup>311</sup> sequence in 4RMBD was investigated; the results are given in Table 1. As a result, it was observed for the first time that the I308A mutant lost its aggregation ability completely, whereas the other mutants still showed aggregation ability, although their ability was reduced to a certain extent. The complete loss of the aggregation ability of the I308A mutant indicates that the close interaction between I308 and Y310 is essential for 4RMBD self-aggregation. The crystal structure [5] of VQIVYK showed a close contact between the side chain of

I308 and the aromatic ring of Y310. This and the present results suggest the importance of an intramolecular C–H···π interaction between both side chains for filament formation. Although a similar C–H···π interaction is possible between Val306 and Tyr308 in the I308Y/Y310A mutant, the lack of notable filament formation indicates that the existence of a C–H group on the N-terminal side with respect to Tyr310 is important for filament formation via a C–H···π interaction.

### 3.2. Importance of C–H···π interaction between I308 and Y310 residues for filament formation of 4RMBD

On the other hand, similar C–H···π interaction to that in wild-type 4RMBD could be expected between the side chains of Y307 and V309 in the potent aggregative Q307Y/Y310A mutant. Although the direction of their side chains is opposite to those of I308 and Y310 with respect to the β-strand <sup>306</sup>VQIVYK<sup>311</sup> plane, the mutual spatial disposition between the V309 side chain and Y307 aromatic ring is the same as that between the side chains of I308 and Y310.

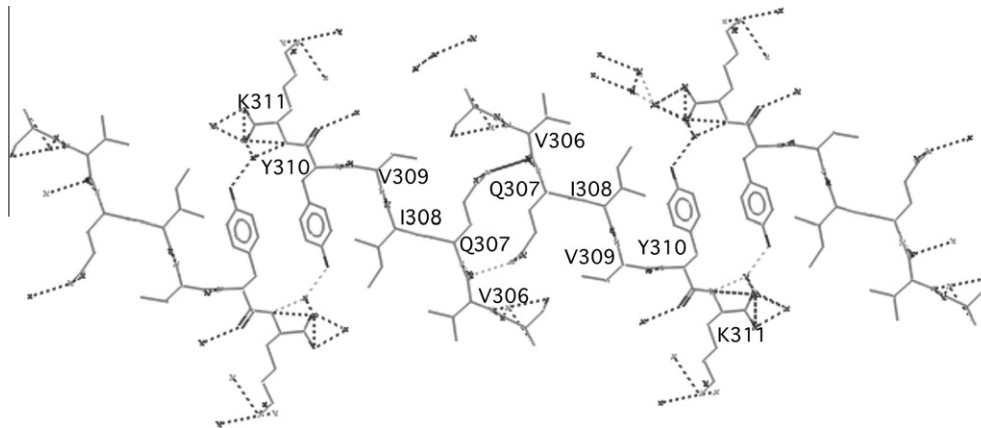


Fig. 3. Probable molecular packing of VQIVYK (305–310) peptide with NNQQNY-like array [11]. The dotted lines represent hydrogen bonds.

If an intramolecular C–H $\cdots\pi$  interaction is essential for filament formation, no aggregation ability of the Q307Y/V309A/Y310A mutant should be expected. To confirm this possibility, the aggregation profile of the mutant was investigated and a complete loss of aggregation was observed, supporting again the importance of the C–H $\cdots\pi$  interaction between I308 and Y310 for the filament formation of 4RMBD. In fact, the importance of this C–H $\cdots\pi$  interaction was confirmed for full-length tau.

### 3.3. General discussion on the role of C–H $\cdots\pi$ interaction in tau filament formation

The C–H $\cdots\pi$  interaction is a kind of hydrogen bond occurring between the C–H donor and the aromatic  $\pi$  acceptor, and contributes significantly to the stability of the three-dimensional structure of a protein [9,10]. Thus, it would be reasonable to consider that this C–H $\cdots\pi$  interaction serves as a “conformational seed” for forming self-aggregation of tau protein. The crystal structure of the tau segment peptide VQIVYK has been used to discuss a model of fibrils of MBD and full-length tau, because it provides a molecular view of the structural organization of the spine of tau fibrils [5]. In the crystal structure, the sequence adopts a  $\beta$ -strand conformation and forms parallel  $\beta$ -sheets with other VQIVYK sequences that combine in a face-to-face interdigitating dry “steric zipper” structure, where the back surfaces between the sheets constitute wet interfaces linked by water molecules. Because no intermolecular close contact between the Y and I residues is formed in the molecular packing of this segment, the intramolecular close contact *via* C–H $\cdots\pi$  interaction is essential for the stabilization of  $\beta$ -strand conformation, which is necessary for the parallel  $\beta$ -sheet formation of the dry “steric zipper” structure.

Interestingly, the molecular packing of the cross  $\beta$ -spine of the GNNQQNY peptide segment from Sup35 [11] appears to be more suitable for interpreting the present aggregation behavior of the tau mutant. Although this fragment forms parallel  $\beta$ -sheets of the face-to-face interdigitating dry “steric zipper” structure similar to those of VQIVYK sequence, the molecular packing in the crystal structure is rather different. Fig. 3 shows a possible molecular packing of VQIVYK taking the same array as that of GNNQQNY. This packing mode can easily interpret why the wild-type 4RMBD, and

the Q307Y/Y310A and Q307Y mutants of 4RMBD exhibit prominent self-aggregation ability. In addition to the intramolecular C–H $\cdots\pi$  interaction, a  $\pi$ – $\pi$  stacking interaction considered to be significant for the self-assembly of fibrils [7,8] is induced between neighboring Tyr residues. Although the mechanism of tau PHF formation has not yet been satisfactorily elucidated, the present work provides important information on the key residue and structural scaffold essential for forming a dry “steric zipper” structure in tau amyloid fibrils.

### References

- Delacourte, A. and Buee, L. (1997) Normal and pathological tau proteins as factors for microtubule assembly. *Int. Rev. Cytol.* 171, 167–224.
- Goedert, M. and Spillantini, M.G. (2000) Tau mutations in frontotemporal dementia FTDP-17 and their relevance for Alzheimer's disease. *Biochim. Biophys. Acta* 1502, 110–121.
- Von Bergen, M., Friedhoff, P., Biernat, J., Heberle, J., Mandelkow, E.M. and Mandelkow, E. (2000) Assembly of tau protein into Alzheimer paired helical filaments depends on a local sequence motif ((306)VQIVYK(311)) forming beta structure. *Proc. Natl Acad. Sci. USA* 97, 5129–5134.
- Von Bergen, M., Barghorn, S., Li, L., Marx, A., Biernat, J., Mandelkow, E.M. and Mandelkow, E. (2001) Mutations of tau protein in front temporal dementia promote aggregation of paired helical filaments by enhancing local beta-structure. *J. Biol. Chem.* 276, 48165–48174.
- Sawaya, M.R., Sambashivan, S., Nelson, R., Ivanova, M.I., Sievers, S.A., Apostol, M.I., Thompson, M.J., Balbirnie, M., Wiltzius, J.J.W., McFarlane, H.T., Madsen, A.O., Riek, C. and Eisenberg, D. (2007) Atomic structures of amyloid cross- $\beta$  spines reveal varied steric zipper. *Nature* 447, 453–457.
- Nishiura, C., Takeuchi, K., Minoura, K., Sumida, M., Taniguchi, T., Tomoo, K. and Ishida, T. (2010) Importance of Tyr310 residue in the third repeat of microtubule binding domain for filament formation of tau protein. *J. Biochem.* 147, 405–414.
- Gazit, E. (2002) A possible role of  $\pi$ -stacking in the self-assembly of amyloid fibrils. *FASEB J.* 16, 77–83.
- Goux, W.J., Kopplin, L., Nguyen, A.D., Leak, K., Rutkofsky, M., Shanmuganandam, V.D., Sharma, D., Inouye, H. and Kirschner, D.A. (2004) The formation of straight and twisted filaments from short tau peptides. *J. Biol. Chem.* 279, 26868–26875.
- Meyer, E.A., Castellano, R.K. and Diederich, F. (2003) Interactions with aromatic rings in chemical and biological recognition. *Angew. Chem., Int. Ed.* 42, 1210–1250.
- Brandl, M., Weiss, M.S., Jabs, A., Suhnel, J. and Hilgenfeld, R. (2001) C–H $\cdots\pi$  interactions in proteins. *J. Mol. Biol.* 307, 357–377.
- Nelson, R., Sawaya, M.R., Balbirnie, M., Madsen, A.O., Riek, C., Grothe, R. and Eisenberg, D. (2005) Structure of the cross- $\beta$  spine of amyloid-like fibrils. *Nature* 435, 773–778.